NJC

Accepted Manuscript

This is an *Accepted Manuscript*, which has been through the Royal Society of Chemistry peer review process and has been accepted for publication.

Accepted Manuscripts are published online shortly after acceptance, before technical editing, formatting and proof reading. Using this free service, authors can make their results available to the community, in citable form, before we publish the edited article. We will replace this *Accepted Manuscript* with the edited and formatted *Advance Article* as soon as it is available.

You can find more information about *Accepted Manuscripts* in the Information for Authors.

Please note that technical editing may introduce minor changes to the text and/or graphics, which may alter content. The journal's standard Terms & Conditions and the Ethical guidelines still apply. In no event shall the Royal Society of Chemistry be held responsible for any errors or omissions in this *Accepted Manuscript* or any consequences arising from the use of any information it contains.

ROYAL SOCIETY OF CHEMISTRY

www.rsc.org/njc

Crystal structures and photocatalytic properties of two novel iodoplumbate hybrids templated by multivalent organic cation

Chao-Hai Wang, [a] **Hai-Juan Du**, [a] **Yao Li**,[a] **Yun-Yin Niu** [a*], **Hong-Wei Hou** [a*]

Abstract: Two novel complexes based on multivalent organic cation and PbI_2 $\{(tbp)_2[Pb_3I_{12}]\}_n$(**1**) (tbp=1,3,5-tri(N-pyridinium methyl)benzene tribromide), $\{(tbpm)[Pb_3I_9]\cdot H_2O\}_n$(**2**) (tbpm=1,3,5-tri(4-methylpyridiniummethyl) benzene tribromide) have been synthesized and characterized by X-ray diffractometry. Compound **1** has a trinuclear structure and compound **2** presents a new 1D iodoplumbate. Photochemical studies reveal the well photocatalytic performances of the two iodoplumbate hybrids. Furthermore, the side chain's effect on the fabrication of iodoplumbate and the photocatalytic performances was also investigated.

Keywords: multivalent organic cation · template effect · photocatalysis · side chain

Introduction

During the last two decades, with the development of global industrialization process, environment pollution becomes more and more serious. Environmental issues have already become the most important problem which influence human survival and development in 21st century.[1] In recent years, photocatalytic reaction has become an ideal environment pollution control and clean energy production technology with its greenhouse depth of reaction and directly using solar energy as the light source to drive the reaction unique performance.[2,3] Among the photocatalyst materials, inorganic–organic hybrid compounds have been considered as one of the most promising photocatalysts. In these hybrids, the inorganic component may confer thermal stabilities and useful functional properties, while the organic component provides designability and multiconfiguration. The combination of these two kinds of components may result in diverse structures and new physical properties. Currently, some results have demonstrated that inorganic-organic hybrid compounds are efficient photocatalysts on the degradation of organic dyes, water splitting, or photoreduction

Dr. C.-H Wang, H.-J Du, Y. Li, Prof. Dr. Y.-Y. Niu, H.-W. Hou.
College of Chemistry and Molecular Engineering, Zhengzhou University, Zhengzhou 450001, P. R. China. E-mail: niuyy@zzu.edu.cn, houhongw@zzu.edu.cn

of CO_2.[4-6] However, how to achieve superior photoactivity, non-toxicity, chemical tability based on inorganic–organic hybrid compounds is still a big challenge.

Our group has been long devoted to the construction of inorganic–organic hybrid compounds and investigation theirs photochemical properties.[7]Although, a series of PbI_2 inorganic–organic hybrid compounds based on monocations and dications have been reported,[8] it is worth to note that iodoplumbate hybrid which templated by multivalent organic cation has never been reported, which may be attributed to the difficulty of controlling and characterization. Multication oriented hybrids may present new interesting topologies because of the existence of multiple interaction sites, and novel functions endowed by host-guest interactions. Herein, we report two low PbI_2 dimension inorganic–organic hybrid compounds, $\{(tbp)_2[Pb_3I_{12}]\}_n$ (**1**) (tbp=1,3,5-tri(N-pyridinium methyl)benzene tribromide), $\{(tbpm)[Pb_3I_9]\cdot H_2O\}_n$ (**2**) (tbpm=1,3,5-tri(4-methylpyridiniummethyl) benzene tribromide), which showed novel and different structures and topologies determined by single-crystal X-ray diffraction analyses and further characterized by infrared spectra (IR), elemental analyses, powder X-ray diffraction (PXRD), and thermogravimetric (TG) analyses. Compounds **1** and **2** show high photocatalytic efficiency on the degradation of methylene blue (MB) and methyl orange (MO) in water under high-pressure mercury lamp irradiation. It is notable that both materials can be used several times without decreasing the photocatalytic efficiency.

Experimental section

Materials and Physical Measurements

The multivalent cations tbp and tbpm (Scheme 1) were prepared as bromides according to the literature,[9] while the other chemicals and solvents were of reagent grade and used as purchased without further purification. The IR spectra were recorded on a Shimazu IR435 spectrometer as KBr disk (4000–400 cm^{-1}). Elemental analyses (C, H, and N) were performed on a Perkin–Elmer 240 elemental analyzer. The UV–Vis diffuse reflectance spectra were measured at UV–Vis–NIR Cary 5000. UV-Vis absorption spectra were obtained using UV-5500 PC spectrophotometer. A

model NETZSCHTG209 thermal analyzer was used to record simultaneous TG curves in flowing air atmosphere of 20mL·min^{-1} at a heating rate of 5 °C·min^{-1} in the temperature range 25–800 °C using platinum crucibles. All powder patterns were collected on a Philips X-pert X-ray diffractometer at a scanning rate of 4 °·min^{-1} in the 2θ range from 5 to 50 ° with graphite monochromatized Cu-Kα radiation (λ=0.15418 nm).

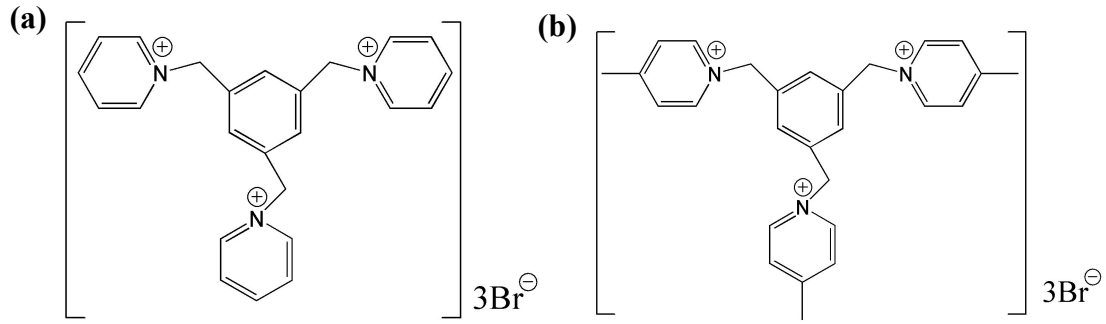

Scheme 1 The title cations tbp (a), tbpm (b)

Synthesis

Synthesis of (tbp)$_2$[Pb$_3$I$_{12}$]}$_n$(1). A suspension of PbI_2 (46.1 mg, 0.1 mmol), tbp (57.6 mg, 0.1 mmol), KI(66.4 mg, 0.4 mmol) in 15 mL of distilled H_2O was sealed in a 25 mLTeflon-lined stainless steel container and heated at 100 °C for 96 h. After the mixture was cooled to ambient temperature at a rate of 10 °C h^{-1}, yellow block crystals of **1** were obtained with a yield of 63% (based on Pb). IR (cm^{-1}, KBr): 3413(w), 3048(w), 2167(s), 1628(s), 1482(w), 1120(m), 1026(w), 751(m), 680(s), 550(m); Anal. Calc: C, 20.20; H, 1.70; N, 2.95%; Found: C, 20.23; H, 1.72; N, 2.89%.

Synthesis of {(tbpm)[Pb$_3$I$_9$]·H$_2$O}$_n$(2). The same synthetic method as that of **1** was used except that tbp was replaced by tbpm (61.8 mg, 0.1mmol). The yield of crystal **2** was 71% (based on Pb). IR (cm^{-1}, KBr): 3443(w), 3041(w), 2167(s), 1636(s), 1462(w), 1157(m), 1028(w), 817(s), 752(s), 592(m); Anal. Calc: C, 14.89; H,1.48; N,1.93%; Found: C, 14.81; H, 1.83; N, 1.96%.

X-ray Crystallography

The crystallographic data for compounds **1-2** were collected on a Bruker SMART CCD diffractometer with graphite-monochromated Mo Kα radiation (λ=0.71073 Å) at 293 K. Absorption corrections were applied by using SADABS. The crystal structures

of **1-2** were solved by the direct method and refined on F2 by full-matrix least-squares techniques with the SHELXTL-97 or OLEX-2 program.[10] All of the non-hydrogen atoms were refined anisotropically. The hydrogen atoms were assigned with common isotropic displacement factors and included in the final refinement by using geometrical restrains. The key crystallographic information for **1-2** are summarized in Table 1. Selected bond lengths and angles are put in Table S1. In order to confirm the phase purity of the bulk materials, Powder X-ray diffraction (PXRD) experiments were carried out for compounds **1-2**, in which the experimental spectra were consistent with their simulated spectra (Fig. S1).

Table 1 Crystal data and structure refinement details for **1-2**

Complexes	1	2
Empirical formula	$C_{48}H_{48}I_{12}N_6Pb_3$	$C_{27}H_{32}I_9N_3OPb_3$
Formula weight	2853.29	2178.23
Crystal system	Monoclinic	Monoclinic
Space group	*P21/n*	*C*c
a/Å	11.140(5)	19.5741(6)
b/Å	23.478(10)	15.1598(5)
c/Å	13.342(6)	15.9810(7)
α(°)	90.00	90.00
β(°)	92.663(5)	97.571(4)
γ(°)	90.00	90.00
V/Å^3	3486(3)	4700.9(3)
Z	2	4
ρ/Mg cm^{-3}	2.719	3.078
μ/mm^{-1}	12.575	16.652
F(000)	2520	3784.0
Crystal size/mm	0.21×0.20×0.16	0.18×0.16 ×0.14
T/K	296(2)	296(2)
Reflections collected	19267	10807
Independent reflections	6138[R(int)=0.0447]	6888[Rint= 0.0363, Rsigma= 0.0619]
data/restrains/ parameters	6138/0/313	6888/41/391
GOF on F^2	1.034	0.992
Final R indices [I>2σ (I)]	R1=0.0413,wR2= 0.1022	R1= 0.0424,wR2= 0.0773
R indices (all data)	R1=0.0571,wR2=0.1105	R1= 0.0620,wR2= 0.0863
Largest diff. peak	1.365	1.53
hole(e Å^{-3})	-2.033	-1.21

Results and Discussion

Synthetic aspects

Hydrothermal treatment of PbI_2 with tbp or tbpm in 1:1 molar ratio and excess KI at 100 °C for 96 h produced **1** (63% yield), **2** (71% yield). In a special hydrothermal process, many factors, such as reactant stoichiometry, pressure, initial reactants, temperature, and reaction time, can affect the formation and crystal growth of the product. The influence of several synthetic parameters on **1-2** is summarized as follows: 1) crystals cann't be obtained without excess KI; 2) a longer reaction time is necessary(>48 h). Compounds **1-2** were stable in air and don't dissolve in water and common organic solvents, such as THF, MeCN, DMF. The elemental analysis was consistent with the chemical formulas. The identities of **1-2** were further confirmed by X-ray crystallography.

Crystal Structure of **1**

This compound crystallizes in the monoclinic system with a space group *P21/n*, and its structure consists $(Pb_3I_{12})^{9-}$ anions and tbp^{3+} cations as shown in Fig.1(a). In the $(Pb_3I_{12})^{9-}$ anion, three Pb atoms in the same line with an Pb–Pb–Pb angle of 180.00 °, which is different from the previously reported equilateral triangle structure $[Pb_3I_{10}]^{4-}$.[11] All the Pb atoms are co-ordinated by iodide ligands in a distorted octahedral fashion. The Pb1 is located in a symmetrical coordination environmen (Pb1-I3=Pb1-I3#1=3.1963 Å, Pb1-I2=Pb1-I2#1=3.2010 Å, Pb1-I1=Pb1-I1#1=3.2342 Å), indicating that the lead(II) center is holodirectional, showing no crystallographic evidence for a stereochemically active lone pair. Whereasy, Pb2 is in an asymmetrical coordination sphere and features a hemidirectional lead(II) center, showing crystallographic evidence for a stereochemically active lone pair.[12] It's very interesting that two I1 atoms and two I3 atoms form a parallelogram (I1#1-Pb1-I1=180.00 °, I3-Pb1-I3#1=180.00 °). The symmetrically two I2 atoms are situated above and below the Pb1 atom, which is the symcenter of the parallelogram (I2#1-Pb1-I2=180.00°). The distance of C-H···I contacts varies from 3.135 to 3.645 Å as shown in Fig. 1(b), which indicating van der Waals interactions or weak H-bonds

happened. The packing in space between inorganic and organic moieties is mainly ascribable to the electrostatic force and van der Waals interactions.

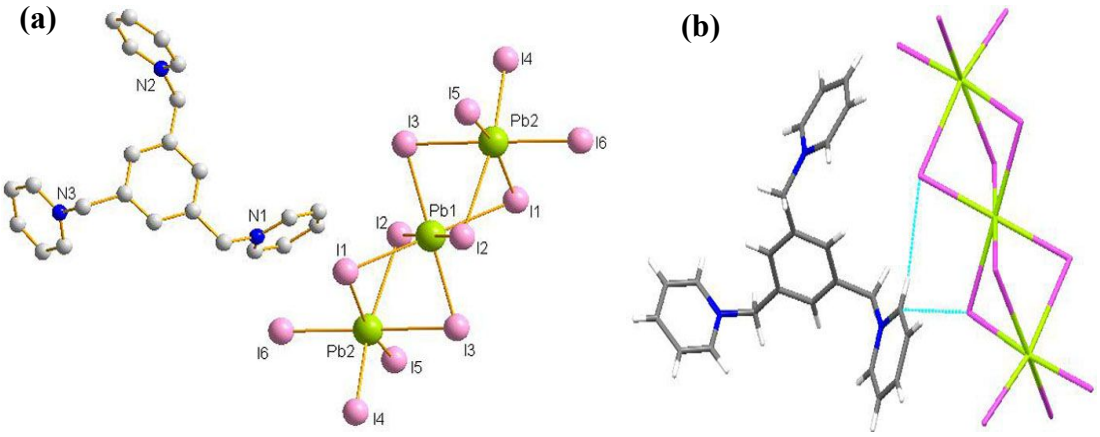

Fig. 1 (a) Molecular structure of **1** and hydrogen atoms have been omitted for clarity; (b) Weak interactions between polyvalent cations and polyvalent anionic. Symmetry codes: #1-x+1,-y+2,-z+1

Crystal Structure of **2**

Compound **2** crystallizes in the monoclinic space group *Cc*, and its structure is composed of 1-D $(Pb_3I_9)^{2n-}$ chains, $tbpm^{3+}$ trications and H_2O molecules. As shown in Fig. 2(a), there are three crystallographically independent Pb atoms (Pb1, Pb2, Pb3). The Pb3 sits on a special position and is coordinated by four I atoms to form a distorted tetrahedron, while (Pb1, Pb2) situated in a slightly distorted octahedral coordination environment. The Pb–I bond distances range from 3.0139(17)-3.3353(14) Å, and the I–Pb–I bond angles fall in the range 78.43(3) to 176.37(4) °. All the lead(II) centers are hemidirectional and the lone pair are stereochemically active. Compared with other reported 1-D chains, $(PbI_5)^{3-}$, $(Pb_2I_6)^{2-}$and (Pb_3I_{10}),[8b,13] this new 1-D iodoplumbate structure type is first reported. It is built up by corner-sharing of (PbI_6) octahedra and trinuclear (Pb_3I_9) clusters. The trinuclear (Pb_3I_9) cluster connects (PbI_6) octahedron through I3, I4, I6 atoms or I1, I5, I8 atoms as shown in Fig. 2(b). Organic cations fill in inorganic framework. Similar with compound **1**, there is the electrostatic and van der Waals contact that acts as the dominant force to hold the hybrid components together. The C-H···I or C-H···C contacts contribute to the packing in space, as shown in Fig. 2(c).

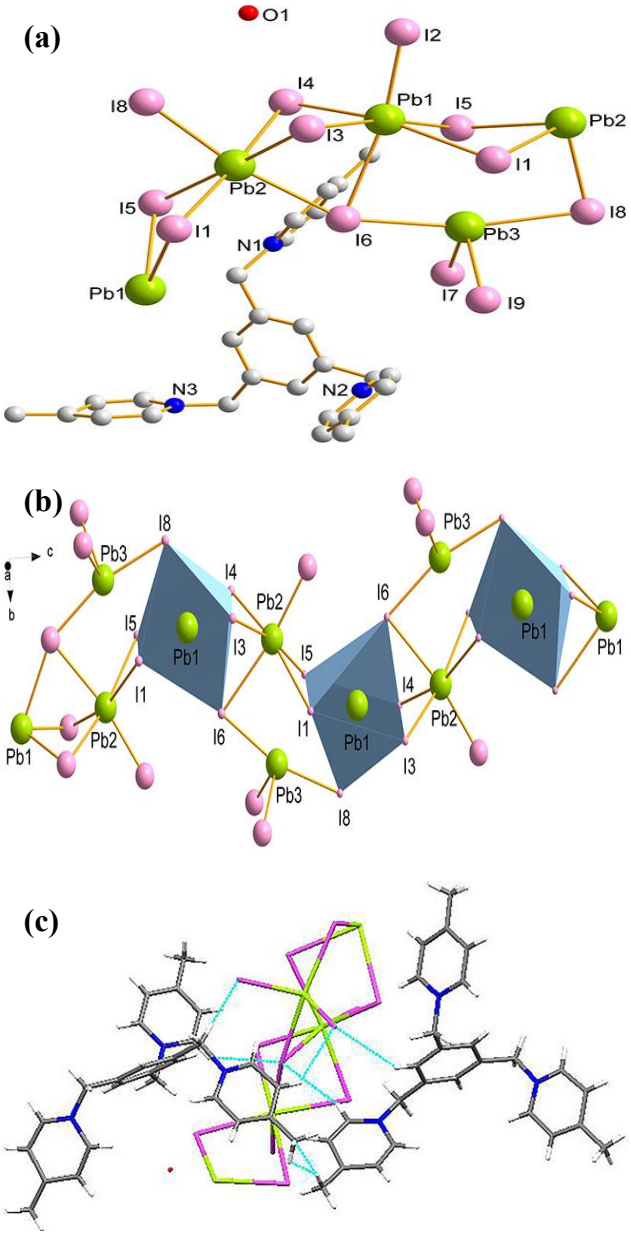

Fig. 2 (a) Structure unit of **2**; (b) The 1D chain of 2 extending along the c-direction; Partial coordination spheres of Pb(II) atoms are shown as polyhedra for clarity; (c) Packing diagram of **1** view along the c axis. Symmetry codes: 1+x,1-y,1/2+z; 2+x,1-y,-1/2+z

Side Chain Effect on the Structure

Compounds **1** and **2** were assembled with PbI_2 and two similar trivalent organic cations tbp and tbpm, however, their anion have markedly different structures. Compound **1** has a trinuclear structure while compound **2** presents a 1D iodoplumbate. Compared the two multivalent organic cations tbp and tbmp, they also possess the same spacer group 1,3,5-tri(methyl)benzene and similar stopper group. The only difference comes from the methyl substituent group on pyridine ring of tbpm. The

structure of compound **2** is more complex than that of compound **1**, which consistent with our previous study results in the aspect of dications: 'template with side-chains favors inorganic composite chains and intricate structures.'[14] This makes our work presented herein to be more reasonable and meaningful.

Thermogravimetry Study

In order to investigate the relation between multiple interactions and the thermostability of compounds **1**–**2**, TG experiments for compounds **1-2** were carried out up to 800°C in flowing air atmosphere and the TG curves are shown in Fig. S1, indicating that the two compounds were almost thermally stable up to 275 °C. Over the range of 275-797 °C, successive weight-loss process corresponds to the decomposition of organic cationic ligand and inorganic bulks. The mass decreased sharply for **1-2** in range of 275 to 345 °C, which probably corresponded to the decomposition of organic cationic ligand (For compound **1,** measured value: 24.85%; calculated value: 23.94%; compound **2,** measured value: 19.03%; calculated value: 19.61); then from 400 °C to 600 °C mainly involved the decomposition of inorganic bulks. By comparing compounds **1-2** with other reported iodoplumbate hybrids which oriented by monocations or dications [8b,8c], compounds **1-2** are more stable that is because there existed multiple interactions in multication oriented hybrids. Similarly, compared with compound **1,** the thermal stability of compound **2** is relative better, which showed that the methyl side-chains may bring more supramolecular interactions between inorganic and organic template moieties.

Optical Band Gap and Photophysical Properties

Optical band gap

Based on our previous research and study results [7b, 7c], we know that the optical band gap (*Eg*) was one principal factor affecting the speed of the photocatalysis degradation process of the organic dye. Illuminated by this, the UV-Vis diffuse reflectance spectra of **1-2** were measured to achieve their band gaps (E_g). The band gaps (E_g) was determined as the intersection point between the energy axis and the line extrapolated from the linear portion of the absorption edge in a plot of

Kubelka-Munk function F against energy E. Kubelka-Munk function, $F=(1-R)^2/2R$, was converted from the recorded diffuse reflectance data, where R is the reflectance of an infinitely thick layer at a given wavelength.[15] Extrapolating the linear par of the rising curve to zero provides the onset of absorption at 2.21eV for **1** and 2.20eV for **2** as shown in Fig. S2, which indicates that these complexes are potential semiconductive materials and possess possible photocatalytic activity.[16]

Photophysical properties

To research in detail the photocatalytic activity of complexes **1-2**, methylene blue (MB) and methyl orange (MO) were selected as models of dye contaminant. The compounds (50 mg) were added into MB (100 mL, 1.0×10^{-5} mol L^{-1}) or MO (100 mL, 5.0×10^{-5} mol L^{-1}) aqueous solution separately. Then magnetically stirred in the dark for 30min to ensure the equilibrium of adsorption/desorption. Afterward, under the irradiation of a 500 W high-pressure mercury lamp the solution was kept continuously stirring with the aid of a magnetic stirrer. 3.0 mL sample was taken for analysis every 15 min. The control experiment was also accomplished under the uniform conditions without any catalyst. The characteristic absorption of MB and MO at about 664 nm (MB) and 463 nm (MO) respectively were chosen to monitor the photocatalytic degradation process as shown Fig. S3-S4. Besides, the concentrations of MB/MO (C) *versus* reaction time (t) of complexes **1-2** are plotted in Fig. 3 (wherein, C_0 is the initial concentration of the MB/MO and C is the concentration of the dye at any given time).

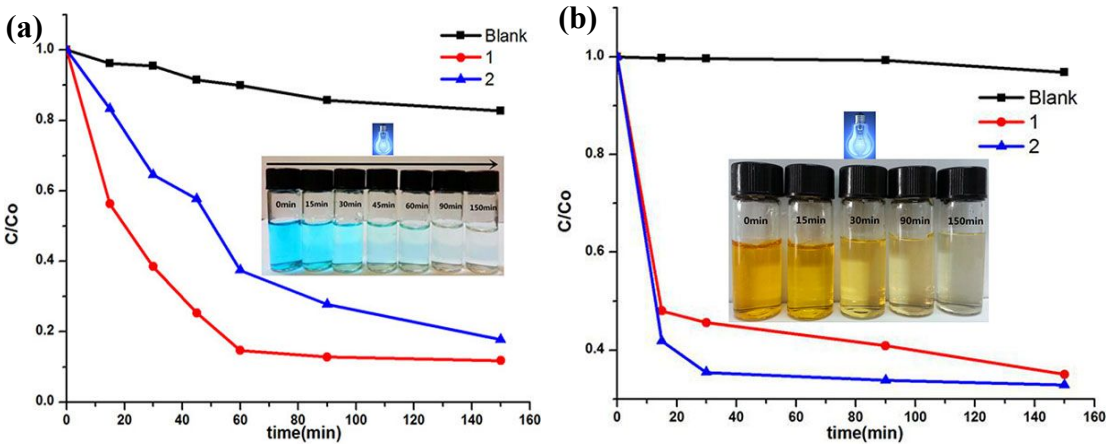

Fig. 3 Photocatalytic decomposition of MB solution (a), MO solution (b) under UV light irradiation with the use of complexes **1-2** and the control experiment without any catalyst

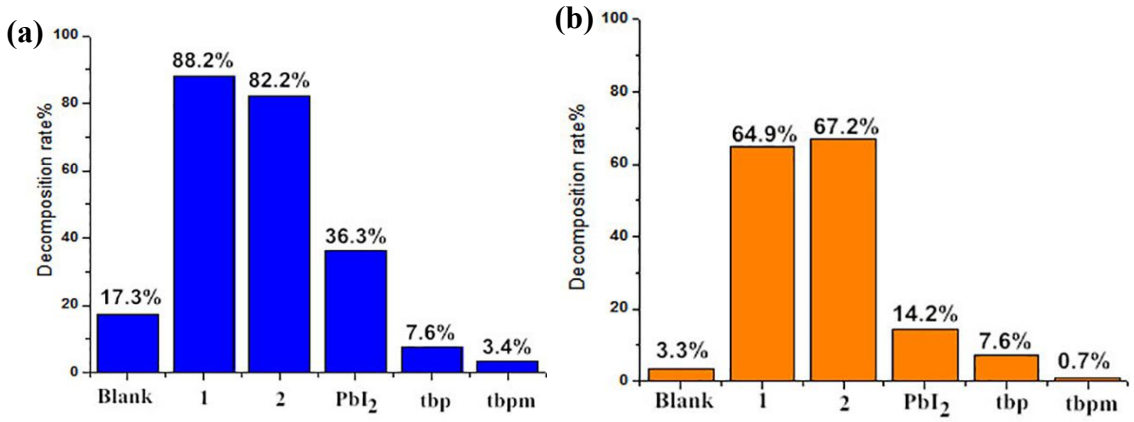

Fig. 4 The degradation rates of MB (a) and MO (b) solutions under the same photodegradation conditions

As shown in Fig. 3, the kinetic data for the degradation of MB is close to first order rate equation, $\ln(C/C_0) = kt$, where k is the rate constant, C_0 and C are the concentration of MB or MO at irradiation time t = 0 and t, respectively.[17] The rate constant k = 0.53 h^{-1} for compound **1**, and k = 0.131 h^{-1} for compound **2**; Similarly, in the degradation of MO, for compound **1** k = 1.15 h^{-1} and for compound **2** k = 1.36 h^{-1} (as shown in **Fig. S6- S7**). On the basis of above photocatalytic results, we can see that complexes **1** and **2** are vigorous for the decomposition of MB/MO under UV irradiation (Fig. 4). It is noted that more than 80% of MB and surpassed 60% of MO have been decomposed during the 150 min with using this two compounds as photocatalys. However, in the same time scope, the control experiments show that the photocatalytic decomposition rate of MB without catalyst is 17.33% and that of MO is 3.25% after irradiation of 150 min. For validating whether photocatalysis originate mainly from the compounds, a negative control test was carried out and the same MB aqueous solution was treated only with the cations or PbI_2 separately. As shown in **Fig. S8-S10**, the cations could hardly accelerate the MB or MO decomposition and the PbI_2 has weak influence on MB decomposition which may because it has a larger band gap.

Probable Degradation Mechanism

As mentioned in the literatures, [6,18] the photocatalytic mechanism is deduced as follows: the electrons (e^-) of complexes were excited from the valence band (VB) to the conduction band (CB). The same number of holes (h^+) that have oxidation

remained in the valence band. These excited electrons can be further captured by O_2 to form superoxide radical anion $\cdot O_2^-$, while the holes can be captured by OH^- to form hydroxide free radical ·OH, which are active species for organic dyes photodegradation (Fig. 5). Commonly, the narrower band gap is conducive to the separation of the charge. As calculated, the band gaps of complexes **1-2** are 2.21 eV and 2.20 eV, respectively. Distinctly, the band gaps of **1-2** defer to the order 2 < 1. For MO, the degradation rate agrees with **2** > **1**, which is perfectly consistent with the theoretical result. However, the degradation rate of MB doesn't agree with the order of the band gaps, which may be influenced by its different positively charged organic component.

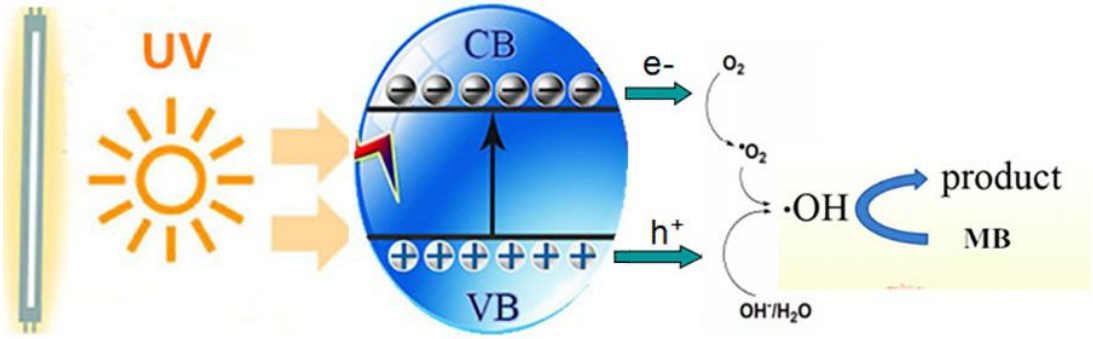

Fig. 5 Schematic diagram showing photocatalytic mechanism

In order to explore whether the ·OH radicals or the holes (h^+) play a major role in the photocatalytic process, compound **1** was selected as the photocatalyst in the degradation research of MB, which is the standard object. EDTA-2Na and isopropyl alcohol (IPA) are often adopted as the traps for holes (h^+) and ·OH in photodegradation reaction, respectively [19]. The experiment to verify the (h^+) and ·OH as active species is the same as the above process except that EDTA-2Na (0.1 mol) or IPA (0.1 mol) was added into the reaction system. As shown in Fig. 6, the degradation of MB is obviously inhibited after addition of EDTA-2Na in reaction system, which implies that the (h^+) species plays chiefly role in the photocatalytic. For the degradation of MO, the negatively charged organic components in it may have a closer interaction to the holes (h^+) and the $tbpm^{3+}$, whereas for the degradation of MB, the positively charged bulk groups in it may be repelled by the holes (h^+) and the $tbpm^{3+}$ with methyl group. So it was considered that steric hindrance and electrostatic

repulsion were the main factors in degradation mechanism.

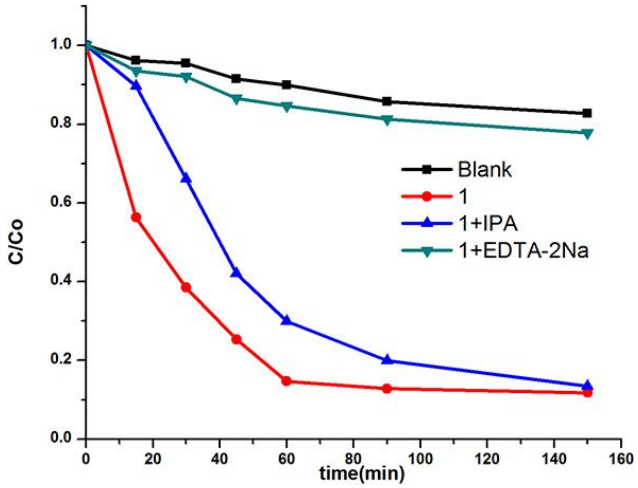

Fig. 6 Activity for MB photodegradation over **1** in the absence & presence of EDTA-2Na and IPA

Although the more elaborate mechanism is also under investigation, the aforesaid phenomenon makes known that **1-2** reveal laudable photocatalytic activities in the degradation of MB/MO under UV irradiation and they may become potential waste-water treatment materials in the future.

Stability and Reuse of the Catalyst

To evaluate the stability of the catalysts, recycling reactions were carried out for the degradation of MB. In each test, the catalyst was separated from the solution use of the centrifugal method (2000 r/min for 10 minutes). Then, filtered and washed with 3×20 ml ethanol, and vacuum-dried at 55 °C. As seen in Fig. 7, the catalyst retained its original activity after repeating the photocatalytic degradation of MB three times. The IR absorption band of the solid residues left in the reaction mixture consistent with that of the two newly synthesized complexes **1**–**2** as shown Fig. 8. As expected, these residues also displayed similar photocatalytic efficiency to that of fresh **1**–**2**, indicating that the stability of compounds **1-2** are very well.

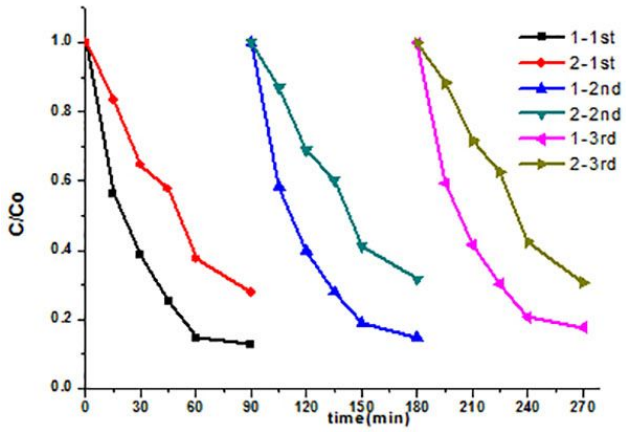

Fig. 7 Recycling test of complexes **1**-**2** for MB photodegradation under light irradiation

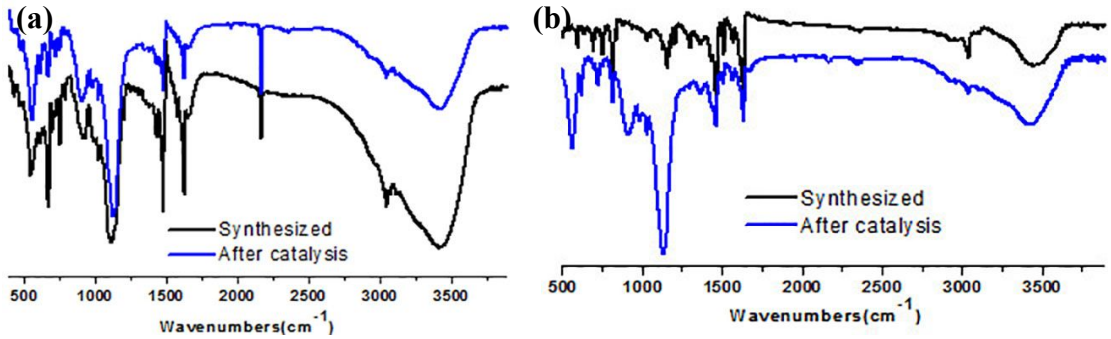

Fig. 8 IR spectras of the prepared and three times repeated samples of **1**–**2** for the photocatalytic degradation of MB (a) for **1**, (b) for **2**

Conclusion

In conclusion, we have first successfully obtained two low dimension iodoplumbate hybrids **1**–**2** templated by multivalent organic cation hydrotherma reactions. The iodoplumbate structures of **1** and **2** are first reported here. Compounds **1**–**2** possess well photocatalytic performances and the catalytic effect was shown to be stable and reusable. Considering their high efficiency and high stability on the photocatalytic degradation of organic dyes, inorganic–organic hybrid materials might be good candidates for photocatalytic applications. This work may paves the way for the preparation of inorganic–organic hybrid materials with new structures and better photocatalytic performances by reasonably designing cationic template. Further studies in this respect are in progress.

Acknowledgements

Research efforts in the Niu group are supported by the National Science Foundation

of China (No. 21171148, J1103309). The Graduate Student Self-innovation Project of Zhengzhou University(14LF00620).

Supplementary material

Supporting information: important bond distances and angles for **1-5**, experimental and simulated powder XRD patterns, spectra data, TGA curves. CCDC reference numbers 1063783-1063784, containing the supplementary crystallographic data for **1-2**. These data can be obtained free of charge via http://www.ccdc.cam.ac.uk/conts/retrieving.html, or from the Cambridge Crystallographic Data Centre, 12 Union Road, Cambridge CB2 1EZ, UK; Fax: t44 1223 336 033 or Email: deposit@ccdc.cam.ac.uk.

Notes and references

[1] (a) A. Kudo, Y. Miseki, *Chemical Society Reviews*, **2009**, *38*, 253-278; (b) K.Tanaka, H. PadermpoIe, T. Hisanaga, *Water Res.*, **2000**, *34*, 327-333; (c) A. L. Linseblgler, G. Liu, T.Yates Jr., *Chem. Rev*.,**1995**, *95*, 735-758.

[2] (a) X .B. Chen, S. S. Mao, *Chem. Rev*., **2007**, *107*, 2891-2959; (b) Y. Sasaki, H. Nemoto, K. Saito, A. Kudo, *J. Phys. Chem. C*, **2009**, 1*13*,17536-17542.

[3] (a) M. P. Fasnacht, N. V. Blough, *Environ. Sci. Technol.*, **2003**, *37*, 5767-5772; (b) H. Tong, S. X. Ouyang, Y. P. Bi, N. Umezawa, M. Oshikiri, J. H. Ye, *Adv. Mater.*, **2012,** 24, 229-251; (c) J. K. Leiand, A. J. Bard, *J. Phys. Chem.*, **1987**, 91, 5076-5083.

[4] (a) F. Wang, Z. S. Liu, H. Yang, Y. X. Tan, J. Zhang, *Angew. Chem., Int. Ed*., **2011**, 50, 450-453; (b) M. C. Das, H. Xu, Z. Y. Wang, G. Srinivas, W. Zhou, Y. F. Yue, V. N. Nesterov, G. D. Qian, B. L. Chen, *Chem. Commun.*, **2011**, 47, 11715-11717; (c) M. Li, L. Liu, L. Zhang, X. F. Lv, J. Ding, H. W. Hou and Y. T. Fan, *CrystEngComm*, **2014**, 16, 6408-6416; (d) L. Liu, J. Ding, C. Huang, M. Li, H. W. Hou and Y. T. Fan, *Cryst. Growth Des.*, **2014**, 14, 3035-3043.

[5] (a) Z. N. Wang, X. Wang, S. Y. Wei, J. X. Wang, F. Y. Bai, Y. H. Xing and L. X. Sun, *New J. Chem*., **2015**, 39, 4168-4177; (b) T. Wen, D. X. Zhang, J. Zhang, *Inorg. Chem*., **2013**, 52, 12-14; (c) H. R. Fu,Y. Kang, J. Zhang, *Inorg. Chem.*,

2014, 53, 4209-4214; (c) M. Dai, H. X. Li , J. P. Lang, *CrystEngComm*, **2015**, 17, 4741-4753.

[6] (a) S. L. Li and X. M. Zhang, *Inorg. Chem*., **2014**, 53, 8376-8383; (b) H. H. Li, X. H. Zeng, H. Y. Wu, X. Jie, S. T. Zheng and Z. R. Chen, *Cryst. Growth Des*., **2015**, 15, 10−13.

[7] (a)Y. Y. Niu, B. L. Wu, X. L. Guo, Y. L. Song, X. C. Liu, H. Y. Zhang, H. W. Hou, C. Y. Niu and S. W. Ng, *Cryst. Growth Des*.,**2008**, 8 2393-2401; (b) H. J. Du, C. H. Wang, Y. Li, Z. C. Yue, L. R. Zhang, L. Li, W. L. Zhang, Y. Y. Niu, H. W. Hou, *Inor. Chim. Acta*, **2015**, 430, 46-54; (c) C. H. Wang , M. Liu , Y. Y. Niu, *Inor. Chim. Acta*, **2015**, 429, 81-86.

[8] (a) Z. J. Tang, A. M. Guloy, *J. Am. Chem. Soc.*,**1999**, 121, 452-453; (b) G. E. Wang, X. M. Jiang, M. J. Zhang, H. F. Chen, B. W. Liu, M. S. Wang, G. C. Guo, *CrystEngComm*, **2013**, 15, 10399-10404; (c) J. M. Yue, Y. Y. Niu, B. Zhang, S. W. Ng, H. W. Hou, *CrystEngComm*, **2011**, 13, 2571–2577.

[9] (a) F. H. Huang, F. R. Fronczek, M. Ashraf-Khorassani and H. W. Gibson, *Tetrahedron Lett*., **2005**, 46, 6765-6769; (b) L. H. Feng, Y. Wang, F. Liang, W. Liu, X. J. Wang and H. P. Diao, *Sens. Actuators, B*, **2012**, 168, 365-369; (c) I. A. Riddell, M. M. J. Smulders, J. K. Clegg, Y. R. Hristova, B. Breiner, J. D. Thoburn and J. R. Nitschke, *Nat. Chem.*, **2012**, 4, 751-756; (d) W. Geuder, S. Hunig, A. Suchy, *Tetrahedran*. **1986**, 42: 1665-1677.

[10] (a) G. M. Sheldrick, SHELXTL-97, Program for Crystal Structure Refinement, University of Gottingen, Germany, **1997**; (b) O. V. Dolomanov, L. J. Bourhis, R. J. Gildea, J. A. K. Howard and H. Puschmann, *J. Appl. Cryst*., **2009**, 42, 339-341.

[11] H. Krautscheid, F. Vielsack, *J. Chem. Soc., Dalton Trans*., **1999**, 24, 2731–2735.

[12] (a) L. S. Livny, J. P. Glusker and C. W. Bock, *Inorg. Chem*., **1998**, 37, 1853-1867; (b) M. J. Katz, V. K. Michaelis, P. M. Aguiar, R. Yson, H. Y Lu, H. Kaluarachchi, R. J. Batchelor, G. Schreckenbach, S. Kroeker, H. H. Patterson and D. B. Leznoff, *Inorg. Chem*., **2008**, 47, 6353-6363. (c) L. H. Zhu, M. H. Zeng, B. H. Ye and X. M. Chen, *Z. Anorg. Allg. Chem*., **2004,** 630, 952-955;

[13] (a) B. R. Vincent, K. N. Robertson, T. S. Cameron and O. Knop, *Can. J. Chem*., **1987**, 65, 1042–1046; (b) D. G. Billing and A. Lemmerer, CrystEngComm, 2009, 11, 1549–1562; (c) A. Okrut and C. Feldmann, *Z. Anorg. Allg. Chem*., **2006**, 632, 409–412; (d) A. Cuna, I. Aguiar, A. Gancharov, M. Pérez and L. Fornaro, *Cryst. Res. Technol*., **2004**, 39, 899–905; (e) G. E. Wang, G. Xu, M. S. Wang, J. Sun, Z. N. Xu and G. C. Guo, *J. Mater. Chem*., **2012**, 22, 16742–16744; (f) S. Wang, D. B. Mitzi, C. A. Feild and A. Guloy, *J. Am. Chem. Soc*., **1995**, 117, 5297–5302.

[14] L. Li, J. M. Yue, Y. Z. Qiao, Y. Y. Niu and H. W. Hou, *CrystEngComm*, **2013**, 15, 3835-3842.

[15] Y. Xia, P. F. Wu, Y. G. Wei, Y. Wang, H. Y. Guo, *Cryst. Growth Des*., **2006**, 6 253-257.

[16] H. Y. Liu, L. Bo, J. Yang, Y. Y. Liu, J. F. Ma, H. Wu, *Dalton Trans*., **2011**, 40, 9782-9788.

[17] L. L. Wen, J. B. Zhao, K. L. Lv, Y. H. Wu, K. J. Deng, X. K. Leng and D. F. Li, *Cryst. Growth Des*., **2012**, 12, 1603-1612.

[18] (a) P. Q. Chen, M. L. Qin, Y. Liu, B. R. Jia, Z. Q. Cao, Q. Wan and X. H. Qu, *New J. Chem*., **2015**, 39, 1196-1201; (b) H. J. Park, W. Kim, W. Choib and Y. K. Chung, *New J. Chem*., **2013**, 37, 3174-3182; (c) S. S. M. Bhat and N. G. Sundaram, *New J. Chem*., **2015**, 39, 3956-3963; (d) H. Kisch, *Angew. Chem. Int. Ed*., **2012**, 51, 2-38.

[19] (a) C. Minero, G. Mariella, V. Maurino, D. Vione, and E. Pelizzetti, *Langmuir*, **2000**, 16, 8964-8972; (b) Y. X. Chen, S. Y. Yang, K. Wang, L. P. Lou, *J. Photochem. Photobiol. A*, **2005**, 172, 47–54.